

Formation and purification of tailored liposomes for drug delivery using a module-based micro continuous-flow system

Nikolay Dimov^{1,+}, Elisabeth Kastner^{2,+}, Maryam Hussain³, Yvonne Perrie³, and Nicolas Szita^{1,*}

¹Department of Biochemical Engineering, University College London, London, WC1H 0AH, UK

²Aston Pharmacy School, School of Life and Health Sciences, Aston University, Birmingham, B4 7ET, UK

³Strathclyde Institute of Pharmacy and Biomedical Sciences, University of Strathclyde, Glasgow, G4 0RE, Scotland

*n.szita@ucl.ac.uk

+these authors contributed equally to this work

ABSTRACT

Liposomes are lipid based bilayer vesicles that can encapsulate, deliver and release low-soluble drugs and small molecules to a specific target site in the body. They are currently exploited in several nanomedicine formulations. However, their development and application is still limited by expensive and time-consuming process development and production methods. Therefore, to exploit these systems more effectively and support the rapid translation of new liposomal nanomedicines from bench to bedside, new cost-effective and scalable production methods are needed. We present a continuous process flow system for the preparation, modification and purification of liposomes which offers lab-on-chip scale production. The system was evaluated for a range of small vesicles (below 300 nm) varying in lipid composition, size and charge; it offers effective and rapid nanomedicine purification with high lipid recovery (>98%) combined with effective removal of non-entrapped drug (propofol >95% reduction of non-entrapped drug present) or protein (ovalbumin >90% reduction of OVA present) and organic solvent (ethanol >95% reduction) in less than 4 minutes. The key advantages of using this bench-top, rapid, process development tool are the flexible operating conditions, interchangeable membranes and scalable high-throughput yields, thereby offering simultaneous manufacturing and purification of nanoparticles with tailored surface attributes.

Introduction

Liposomes are a well-established formulation strategy to improve drug delivery and enhance therapeutic outcomes for a range of drugs, such as pharmaceuticals, biopharmaceuticals, and vaccines. Due to their bilayer vesicle structure, which is akin to natural cells, liposomes are able to incorporate drugs both within their aqueous core and their lipidic bilayers. Through such means, the pharmacokinetics of a drug can be controlled and dictated by the liposomal delivery system rather than the drug attributes. This has allowed the development of a range of clinically approved liposome-based medicines including DOXIL/Caelyx® (doxorubicin), AmBisome® (amphotericin B) and Daunoxome® (daunorubicin), which when combined have an annual market revenue of approximately \$100 million. However, despite these advantages, their wider application is limited by their complex and costly production requirements. Currently, manufacturing methods include the use of solvent injection, reverse-phase evaporation and emulsification methods¹. Such methods have the disadvantage of involving multi-step processes, often adopt large amounts of organic solvents and are limited to batch-release processes. Furthermore, a crucial attribute to an effective liposomal drug system is the vesicle size range, which can be controlled the production method, e.g. sonication (20-40 nm)², extrusion (70 - 415 nm)³ or high-pressure homogenisation (20 - 140 nm)⁴; and, more recently, microfluidic mixing (20 - 80 nm)^{5,6} or flow focusing (50 - 150 nm)⁷. Upon administration, the pharmacokinetic profile and fate of liposomes is dictated by their size and therefore controlling particle size and polydispersity (PDI) is a key issue in their manufacturing and a key parameter in the product specifications. To produce liposomes in a controlled size range, downsizing through extrusion or homogenisation is often adopted. This adds further steps to the manufacturing process and exposes the liposomes and drug constituents to harsh and potentially detrimental processing conditions. To address these issues, and allow the wider adoption of liposomal systems to improve health-care, new methods in liposome manufacture are therefore required.

Microfluidic devices operate with small volumes, offer exquisite control over the fluid flow^{8,9}, and make efficient use of materials, reagents and energy¹⁰. These advantages have been applied for the reproducible

58 formation of liposomes with uniform size distribution^{1, 6, 11}. Typically, liposome formation occurs at the
59 interface of an aqueous and a solvent phase, containing lipid molecules¹², and microfluidic devices are well
60 suited to establish and finely control such interfaces. In hydrodynamic flow focusing (HFF) devices, for
61 example, where the solvent phase is microinjected in between two co-flows of aqueous buffer, liposomes
62 with well-controlled size distributions can be assembled^{6, 13}. Furthermore, by changing the ratio between the
63 flow rates of the aqueous buffer and organic phase, the concentration of lipid molecules in the organic
64 phase, or by adapting the channel geometry, the size of the liposome can be finely prescribed^{14, 15}. Scaling
65 up of HFF devices, however, is difficult which constrains the amount of liposomes that can be produced per
66 unit time¹⁶. In contrast, devices based on chaotic advection micromixing^{11, 17} are more suitable for high
67 throughput production of liposomes. Lipid nanoparticles with sizes between 20 and 50 nm were reported
68 using a staggered herringbone mixer (SMH) by varying triglyceride ratios⁵. More recently, Kastner et al. used
69 the same SMH to prepare liposomes encapsulating propofol¹⁸, a poorly water-soluble drug. These works
70 demonstrate the potential application of microfluidics for the rapid, reproducible and size-controlled formation
71 of drug-loaded liposomes.

72
73 Purification remains a significant hurdle in the development of liposomal products. Irrespective of which
74 production method is adopted, non-entrapped contaminant molecules, small molecule drugs or proteins must
75 be removed from the final liposome product. Separation is typically achieved by filtration^{19, 20} or ultra-
76 centrifugation, which can be challenging for the large-scale purification. Other possible routes for removal of
77 non-encapsulated material include dialysis, gel-permeation chromatography, ion-exchange chromatography,
78 and size exclusion chromatography. However, these processes are time-intensive and can furthermore
79 diminish product yield by column equilibration, which dilutes the final liposomal product, even with size
80 exclusion chromatography²¹.

81
82 To address these issues of post assembly refinement, here we investigate a 'lab-on-chip' module-based
83 microfluidic manufacturing and purification system for the production of liposomes. In contrast to previously
84 reported on-chip devices by other groups and by us^{5, 18, 22, 23}, where lengthy dialysis procedures for removal
85 of non-entrapped drug and solvent residues were required, we present a novel continuous microfluidic
86 liposome production and purification process train which generates purified liposomal products in less than 4
87 minutes. Furthermore, the purification step is based on a tangential flow-filtration device with an easily
88 exchangeable membrane, allowing therefore the purification of a broad variety of liposome formulations. This
89 robust process train facilitates the identification of prospective formulations, optimal operating conditions and
90 scale-up parameters, whilst significantly reducing the time required for developing versatile adjuvant and
91 drug delivering systems.

92 93 94 **Results**

95
96 In order to obtain a continuous microfluidic liposome production and purification process train, we first
97 characterised a tangential flow filtration (TFF) device²⁴ and its purification capabilities for a variety of
98 liposome formulations using lipids as outlined in Table 1.

99 100 **On-chip purification of liposomes for determination of the range of operational transmembrane** 101 **pressures**

102
103 To identify the operational backpressure which yields the maximal recovery, we introduced in to the TFF
104 device a commonly used formulation of neutral liposomes (PC:Chol; 1:1 molar ratio; Table 1). By varying the
105 flow rates, and by implementing capillaries with different inner diameters and lengths downstream of the TFF
106 device, we investigated backpressures from 7 to 80 psi (Table 2). To assess the liposome retention on the
107 retentate side of the membrane (the volume of the liquid, which does not pass through the membrane), we
108 collected samples from both the retentate and permeate (the volume which passes through the membrane),
109 and measured the liposomal size and polydispersity index (PDI) at each of the backpressure conditions. The
110 results (Fig. 1) show that there was no significant change in the size (approximately 115 nm) and PDI (0.15)
111 of the liposome suspension in the retentate across the pressure range tested. However, at backpressures of
112 75 psi and 80 psi, particles were detected in the permeate as confirmed by qualitative image-based
113 nanoparticle tracking analysis NTA (Fig. 1). To confirm membrane integrity and exclude membrane damage
114 as a possible cause for the liposome transferred into permeate, a leak-test applying pressures higher than 80
115 psi was run and confirmed the membrane was intact. This suggests that at pressures above 75 psi, the TFF
116 device was unable to retain liposomes and these were being pushed across the membrane into the retentate
117

The effect of filtration on particle characteristics of cationic and anionic liposomes

After proving that neutral PC:Chol liposomes were retained, the application of the TFF to purify cationic (DDA:TDB; 8:1 molar ratio; Table 1) and anionic liposomes (DPPC:Chol:DPPG; 4:4:1 molar ratio; Table 1) was assessed (Fig. 2). The TFF device was first challenged with a batch-formulated cationic liposomal adjuvant (DDA:TDB) in three diafiltration cycles with buffer replenishment after each cycle, compensating for the volume of liquid passing into permeate. At a flow rate of 1 mL min⁻¹, the backpressure was 49 psi (capillary length 50 mm, and I.D. 100 µm, Table 2), yielding a calculated flow rate of water through the cellulose membrane, $Q_{\text{transmemb}}$, of 0.25 mL·min⁻¹ (based on a linear extrapolation from supplier data; 16 mL min⁻¹ cm⁻² for 14.5 psi).

With the cationic liposomes, the particle concentration of liposomes was 4.1 x 10⁹ P/mL, which reduced to 3.8 x 10⁹ P/mL at the end of the third cycle (Fig. 2A) confirming the yield from the filtration process was 93% for the cationic liposomes. With these systems the liposomal size (approximately 300 nm) and cationic nature (approximately 60 mV) were not notably influenced by the filtration process (Fig. 2A). Furthermore, NTA analysis (Fig. 2B) showed that there were no cationic liposomes detected in the permeate.

Similar results were demonstrated with anionic liposomes; filtration of batch-formulated anionic liposomes (DPPC:Chol:DPPG) using three diafiltration cycles produced no notable changes in terms of vesicle size (approximately 120 nm), PDI (0.14 to 0.15), ZP (-55 mV) and particle concentration (4.4 to 4.6 x 10¹⁰ P/mL) (Fig. 2). As with the neutral and cationic liposomes, NTA analysis in each diafiltration cycle verified that no liposomes were present in the permeate (Fig. 2B).

Purification of non-incorporated drugs from liposome formulations

Having successfully demonstrated the capability of the TFF to retain a wide range of different liposome systems, we then focused on investigating the efficiency of the TFF to purify the liposomal nanomedicines and remove non-incorporated drug (RC membrane, 10 kDa cutoff). To study drug removal, propofol (1 mg·mL⁻¹) was added to a suspension of negatively charged liposomes (DPPC:Chol:DPPG) in aqueous solution containing 20% (v/v) ethanol residual solvent levels found after liposome production by microfluidics prior to purification. Propofol, was employed as it has previously been studied as a low-solubility drug solubilised within liposomes. The TFF was shown to effectively purify the liposomes by removing both the solvent and non-incorporated drug with 90 % of the non-incorporated propofol being removed in the first diafiltration cycle, with a further removal of 80% in the second diafiltration run, and a further 60% after the third diafiltration cycle (Fig. 2C). Thus, after three cycles only 1% of the 'free' non-incorporated drug remained within the formulation (Fig. 2C). Simultaneously, the TFF system removed the ethanol which had been used for the liposome formulation (Fig. 2C). Ethanol was reduced by approximately 50% in the first diafiltration cycle, and after three diafiltration cycles the residual ethanol concentration was 3% (v/v) (Fig. 2C).

Purification of 'free' protein from liposome formulations

To investigate the removal of non-entrapped protein from liposome formulations, both cationic (DDA:TDB) and anionic liposomes (DPPC:Chol:DPPG) were considered given that electrostatic interactions between cationic liposomes and anionic proteins is exploited in the loading of antigens to liposomal adjuvant systems. Therefore both liposome systems were mixed with ovalbumin (OVA; 100 µg mL⁻¹). At a flow rate for the retentate of 2.5 mL min⁻¹, the backpressure was 62 psi (capillary length 25 mm, and I.D. 100 µm, Table 2), yielding a calculated flow rate of water through the PES membrane (MWCO 300 kDa), $Q_{\text{transmemb}}$, of 1.69 mL·min⁻¹ (based on a linear extrapolation from supplier data; 58 mL min⁻¹ cm⁻² for 10 psi). Thus, from 2.5 mL initial sample only 0.81 mL remain in the retentate fraction, and 1.69 mL pass through the membrane. The theoretical volume of permeate accounted for 67% of the initial liquid.

Given the anionic nature of OVA at the pH range used, electrostatic interactions with the cationic but not the anionic liposomes occurred. Indeed, anionic liposomes maintained a similar size (approximately 120 nm) after the addition of OVA (Fig. 3A); however, for the cationic liposomes, the electrostatic interactions with the anionic OVA resulted in aggregation and in an increased vesicle size from around 220 nm to 300 nm, and a drop in their cationic nature from 59.8 ± 1.9 mV to 17.5 ± 1.4 mV (Fig. 3B).

After the addition of protein, both systems were subjected to three diafiltration cycles. The size and PDI of both the anionic (Fig. 3A) and cationic (Fig. 3B) liposomes were not significantly altered through the course

178 of the diafiltration cycles and particle recovery was 87% and 96%, respectively (Fig. 3). Protein (OVA) and
179 residual ethanol was removed into the permeate stream over the three diafiltration cycles, with a final
180 removal of 70% of the free protein and 95% of the solvent with the anionic liposomes (Fig. 3C). Similar
181 results were achieved with the cationic liposome systems (Fig. 3D); by using TFF purification, ethanol
182 residues were reduced to 4% (v/v) of the starting value and 75% protein was removed (Fig. 3B) after three
183 diafiltration cycles. The reduced levels of protein removed from the cationic system were a result of protein
184 loading onto the surface of the liposomes due to electrostatic interactions (but not related to the filtration
185 process in the TFF).
186

187 **Micro continuous-flow system for production, modification and purification of liposomes**

188

189 Having established the efficacy of the TFF purification system, the next stage was to develop a continuous
190 manufacturing and purification process for liposomes. To achieve this, a staggered herringbone micromixer
191 (SHM) was employed to generate the liposomal systems and directly feed the TFF device with the
192 liposomes. To optimise the throughput for each of the two devices separately, and to independently control
193 the flow rates, an intermediate collection vial was used (Fig. 4). Furthermore, the intermediate collection vial
194 allowed purification of the liposomes in diafiltration mode. After each diafiltration cycle, fresh buffer was
195 added manually into the intermediate vial to compensate for the volume passing through the membrane into
196 the permeate. Continuous production (Fig. 4) was demonstrated by using 1) neutral liposomes (PC:Chol, 4:1
197 molar ratio) with propofol and 2) cationic liposomes (DOPE:DOTAP, 1:1 molar ratio; Table 1) loaded with
198 surface-complexed protein. Lipid recovery after 4 diafiltration cycles remained at 100%, matching the initial
199 amount of lipids present prior to TFF (Fig. 5A). Without buffer replenishment, the system performed
200 concentration cycles for formulations (Fig. 5B). Within four cycles, the concentration of lipids measured in the
201 retentate doubled (Fig. 5B). This was due to a 50% reduction in volume as the overall quantity of lipids in the
202 retentate remained constant, matching the lipid content after the SHM (but before the TFF).
203

204 **Continuous manufacture and purification of liposomes with bilayer loaded drug**

205

206 This system was then applied for the continuous manufacture and purification of liposomes incorporating
207 propofol (Fig. 4B). Liposome (PC:Chol) production and drug encapsulation were performed in a staggered
208 herringbone mixer (SHM), operated with a volumetric flow rate of 2 mL min⁻¹ and a 1:3 solvent:aqueous
209 buffer ratio. The resulting liposomes were 50 nm in size with a PDI of 0.3 (Table 3) in line with previously
210 reported studies²⁵. Using the continuous manufacturing set up (with three diafiltrations), liposomes were
211 therefore both manufactured and purified. This continuous system was able to produce a purified liposome
212 product incorporating 51 mol% propofol (in line with previously reported drug loading achieved using a 2 step
213 manufacture and purification process based on dialysis¹⁸), with clinically acceptable ethanol levels (3% (v/v);
214 Table 3). Furthermore, liposomes manufactured and purified in this continuous systems retained their
215 physico-chemical attributes and were not significantly different in size, nor PDI from those not subjected to
216 TFF purification (Table 3). Examples of electron microscopy images of liposomes are shown in
217 Supplementary Figures S1 and S2.
218

219 To compare the characteristics and drug loading of PC:Chol liposomes loaded with propofol, the same
220 formulation was prepared using hand-held extrusion (10 passes through a 400 nm, 200 nm, 100 nm and final
221 50 nm pore size filters). Whilst this method of liposome manufacture was not the main focus of this study and
222 could be further optimized, again these liposomes were effectively purified to remove free drug using TFF
223 (with drug loading of 3.6 ± 0.38 mol %; data not shown) and the liposome size and PDI remained unchanged
224 by TFF purification (107.9 ± 14.1 nm and 109.9 ± 19.0 nm with PDI values of 0.17 ± 0.10 and 0.34 ± 0.06 pre
225 and post TFF purification respectively, results not shown).
226

227 **Continuous manufacture and purification of cationic liposomes with adsorbed protein**

228

229 The lab-on-chip micro continuous-flow system was next challenged with the production of cationic
230 (DOPE:DOTAP) liposomes, which were modified with added ovalbumin in the intermediate connection vial
231 and finally subjected to purification (Fig. 4C). Lipids were included in the ethanol stream and liposome
232 formation was performed using the SHM, which operated at 2 mL min⁻¹ and a 1:3 solvent:aqueous buffer
233 ratio. The outflowing liposome solvent mixture was collected in the intermediate collection vial after 1 minute
234 of SHM operation, and analysed (size, PDI, ZP). The resulting liposomes had a size of 62.8 ± 1.9 nm, PDI of
235 0.4 ± 0.02 and ZP of 84 ± 3.5 mV prior to addition of OVA. Then ovalbumin was added to the intermediate
236 vial, resulting in vesicles with a larger size (88.5 ± 5.7 nm), unaltered polydispersity (0.45 ± 0.01), and
237 reduced ZP (43.6 ± 1.6 mV) (Table 4), again as a result of interactions between the cationic liposomes and

238 the anionic protein. After manufacture and purification on the system, liposomes were unaltered in size (89.3
239 \pm 10.9 nm; PDI 0.42 \pm 0.02) and had an increased ZP (69.2 \pm 6.1 mV) (Table 4), presumably through the
240 purification and removal of 74% 'free' protein from the system. Residual solvent levels were also reduced to
241 clinically acceptable levels (4 %; Table 4). Examples of electron microscopy images of liposomes are shown
242 in Supplementary Figure S1.
243

244 Discussion

245
246 We successfully investigated the region of operation for the Tangential Flow Filtration (TFF) device with
247 various liposome formulations and confirmed the upper limit of operational pressure for the presented
248 purification system to be 75 psi. A pressure range between 5 and 80 psi is a common backpressure
249 implemented in industrial filtrations²⁶ which is virtually identical to our TFF. During pressure tests, the
250 membrane remained intact throughout, and therefore it can be considered that the measured backpressure
251 equaled the transmembrane pressure inside the TFF. This transmembrane pressure could be adjusted
252 accordingly using the data available in Table 2; alternatively, it could be calculated from Hagen Poiseuille's
253 equation. Based on these findings we determined the optimal operational transmembrane pressure of 62 psi,
254 which corresponded to a maximum flow rate of 2.5 mL min⁻¹ through a restrictive capillary with an internal
255 diameter of 100 μ m and a length of 25 mm. At this flow rate, our sample (2 mL) took less than a minute (~48
256 s) to run through the system, which shows a distinct advantage over the current methods that require lengthy
257 bench-top, post-synthetic dialysis²². At high shear rates, drug release from liposomes can be a problem.
258 However, the calculated average shear rate at the maximum flow rate of 2.5 mL min⁻¹ inside the retentate
259 channel is approximately 590 s⁻¹ (Supplementary Information S3). This value is lower than previously
260 reported shear rates²⁷ of 800 s⁻¹ for which no influence on the permeability or integrity of the liposome
261 membranes was found. Furthermore, the flow rates matched those previously applied for liposome
262 manufacturing using a device with a SHM^{5, 25}. Thus, we proved that a SHM can be coupled directly with the
263 TFF, and that we could generate and purify liposomes in a continuous mode without any losses into the
264 permeate. Overall our results show that our filtration system can be implemented for multistage purification of
265 a broad range of liposomal products.
266

267 Backpressures of 75 psi and higher, however, led to losses of liposomes through the intact cellulose
268 membrane into the permeate. One possible explanation could be that of particle extrusion across the
269 membrane at these high pressures. It is well known that liposomes can undergo extrusion through cylindrical
270 pores in membranes. Industrial scale extrusion tends to use higher lipid concentration than in our current
271 study and adopts higher pressures ranging between 100-700 psi. However, extrusion of liposomes is system
272 dependent; polycarbonate filters are used at pressures less than 100 psi, and low lipid concentrations
273 require lower pressure²⁸. Therefore, to avoid extrusion, a backpressure of 75 psi was adopted as the critical
274 cut off value. Membrane characteristics also play an important role for liposome recovery as they influence
275 the flux from the retentate to the permeate. The calculated transmembrane flow was 0.32 mL min⁻¹ (or 12.8%
276 of the total flow rate, TFR) for a hydrophilic membrane with a pore size of 0.22 μ m, at a backpressure of 62
277 psi and nominal flow rate of 2.50 mL min⁻¹ (retentate). In contrast, for the same backpressure and same
278 nominal flow rate, a membrane with a 0.45 μ m pore size resulted in a transmembrane flux of 1.69 mL min⁻¹,
279 corresponding to 67.6% of the retentate inflow. Furthermore, the presented setup demonstrates that a range
280 of capillaries with varying inner diameter and length can be applied to control the backpressure and the
281 dilution or concentration rates of the system, allowing to tailor resulting flow rates and to adjust throughputs.
282

283 Having established optimal operational conditions of our TFF device, its purification capacity for the removal
284 of non-incorporated hydrophobic drug (propofol) and residual ethanol was studied. Over three diafiltration
285 cycles, the quantity and quality of liposomes were preserved after purification for the anionic vesicles. For the
286 cationic liposomes, there was a small increase in polydispersity, but no significant increase in liposome size
287 (Fig. 2A). The propofol content decreases much faster in comparison to the ethanol (Fig. 2B), with the
288 hydrophilic membrane (0.22 μ m pore size). This could potentially be due to capillary action that channels the
289 separation of lipophilic propofol²⁹ (Log K_{ow}=3.79) through the membrane. The ethanol content was the critical
290 factor, which determined the required number of diafiltration cycles. After three diafiltration cycles, only 1% of
291 non-incorporated propofol and 3% residual ethanol remained within the liposomal suspension with no
292 changes in liposome physico-chemical attributes or concentration (Fig. 2) demonstrating the ability of this
293 system to provide liposomes purified to a level as would be expected for a therapeutic product.
294

295 In terms of removal of non-associated protein from liposomes, as might be required for liposomal adjuvants
296 or biological therapeutics, protein removal is challenging because high concentrations of protein can lead to
297 membrane fouling due to protein-membrane interactions²⁴. Such protein-membrane interactions occur due to

298 electrostatic repulsion forces. Similar to propofol removal, the dilution by replenishing with fresh buffer, and
299 subsequent filtration facilitates the reduction in concentration of free protein in the retentate. Purification
300 therefore occurs as a result of two cumulative effects: one from the separation at the membrane and the
301 other from the dilution of the retentate. As demonstrated, separation can be controlled by adjusting flow rates
302 and restrictive capillary sizes; also by varying the amount of liquid that is replenished after each diafiltration
303 cycle. In our results, the volume amounted to the volume of the permeate, thus maintaining constant the
304 amount of liquid circulating in lab-on-chip purification system.
305

306 The tolerated levels of free protein depend on the requirements implied by the target application of the
307 liposomes and the number of diafiltration cycles can be adjusted accordingly to match those criteria for
308 purity. A particular focus in the delivery of protein antigens is the use of cationic liposomes, with electrostatic
309 attractive forces dominating and often leading to a surface-adsorption reaching close to 100% depending on
310 protein concentrations used³⁰ and purification can further be complicated by the cross-linking and/or
311 aggregation of cationic liposomes (DDA:TDB) with protein. We have demonstrated the capability of the
312 filtration device to separate non-adsorbed ovalbumin (OVA) from a cationic liposome formulation and
313 residual solvent with high liposome adjuvants recovery (87%) (Fig. 3). This presents compelling evidence
314 that our micro continuous-flow purification device, i.e. TFF device, is capable of providing an effective post-
315 production purification step, with the option to recycle purified protein for subsequent applications.
316

317 The liposome process flow system presented here (Fig. 4) facilitates the complete removal of the free drug,
318 which was previously only achievable by time intensive, bench-top dialysis^{18, 22}. The encapsulation and
319 solubilisation of drug with low aqueous solubility in the bilayer of liposomes has been investigated previously
320 using a microfluidics based system¹⁸. In that study the assembly of PC:Chol liposomes was performed using
321 a SHM, and the method was established as a robust, reproducible approach for preparing size-controlled
322 liposomes as solubilising agents. The same SHM is implemented in this herein reported system to
323 investigate the effects of continuous processing on drug encapsulation by measuring amounts of drug
324 encapsulated in the liposome bilayer. Very importantly, the amount of encapsulated drug and physical
325 characteristics (size, PDI) show that continuous processing and the pressures applied in the TFF have no
326 adverse effect on liposome integrity (Table 3). The presented assembly utilizes the methanol solubilisation
327 as the initial step of liposome production. However, it is possible to replace time-intensive production and
328 dialysis (hours) with a micro continuous-flow system (minute-long process) manufacturing and purification to
329 rapidly remove residual solvent. Among the main merits of using the continuous microfluidic process flow are
330 the mild conditions during the assembly of the liposomes and the replacement of long ultracentrifugation
331 steps for protein removal³¹. It can be concluded that the performance of the process flow system
332 demonstrated (Fig. 4) for liposomes is consistent with: (i) the results from the stand-alone SHM in terms of
333 particle characteristic; (ii) the results from the stand alone TFF in terms of purification.
334

335 **Conclusions**

336
337 We have successfully demonstrated for the first time the feasibility for on-chip purification of liposomal
338 batches for process development. Liposome manufacture, drug loading and removal of contaminants (such
339 as un-entrapped drug or protein as well as solvent residues) were performed in a continuous mode using two
340 microfluidic devices, allowing for manufacturing, purification and concentration of liposomal drug products.
341 These devices were successfully challenged with a range of liposomes, varying in lipid composition, surface
342 potential, size and concentration. The results demonstrate the ability of the on-chip filtration unit to be
343 tailored to a broad diversity of lipid-based nanoparticles by varying the operational parameters. The
344 microfluidic devices allow for an efficient and quick investigation of several lipid or drug candidates, and meet
345 high throughput requirements of early stage development processes. The continuous process may permit
346 determination of liposomal characteristics (e.g. size, surface potential, particle number) and encapsulation
347 efficiencies of a wide variety of drug molecules, allowing for future integration of process analytical
348 technologies (PAT) to further aid reproducibility. Furthermore, the setup is of considerable interest for cost-
349 intensive drugs or protein encapsulation development, as the process requires micro volumes. The
350 microfluidic device developed herein can cope with a variety of proteins developed by the biopharmaceutical
351 industry. The device has the flexibility of integrating different types of membranes to cater for a variety of
352 uses; also has the option of scalability through parallelization of the mixer chips and TFF membranes, and
353 thereby can be easily translated to industrial setting³².
354

355 **Methods**

357 Chemicals

358

359 Egg Phosphatidylcholine (PC), CAS: 8002-43-5, 1,2-Dipalmitoyl-*sn*-glycero-3-phospho-*rac*-(1-glycerol)
360 sodium salt (DPPG), CAS: 67232-81-9, 1,2-Dipalmitoyl-*sn*-glycero-3-phosphocholine (DPPC), CAS: 63-89-8
361 and Cholesterol (Chol), CAS: 57-88-5 were obtained from Sigma-Aldrich Company Ltd. (Poole, UK). 1,2-
362 dioleoyl-*sn*-glycero-3-phosphoethanolamine (DOPE), CAS: 4004-05-1, 1,2-dioleoyl-3-trimethylammonium-
363 propane (DOTAP), CAS: 144189-73-1, dimethyldioctadecylammonium bromide (DDA), CAS: 3700-67-2 and
364 trehalose 6,6-dibehenate (TDB), CAS: 66758-35-8 were purchased from Avanti Polar Lipids, Inc., (Alabaster,
365 AL), purity >99% (Table I). Ethanol, CAS: 64-17-5, and methanol, CAS: 67-56-1, were obtained from Fisher
366 Scientific (Loughborough, UK). TRIS Ultra Pure, CAS: 77-86-1, was obtained from ICN Biomedicals, Inc.,
367 (Aurora, Ohio). Propofol (2,6-Bis(isopropyl)phenol), CAS: 2078-54-8 and ovalbumin (chicken egg), CAS:
368 9006-59-1 were obtained from Sigma-Aldrich Company Ltd., (Poole, UK). Ultrafiltration regenerated cellulose
369 membranes (p/n: U2755-10AE) were obtained from Sigma-Aldrich Company Ltd., (Poole, UK) (10kDa, pore
370 size 0.22 μm), and Biomax polyethersulfone ultrafiltration membrane discs with 300 kDa cutoff, pore size
371 0.45 μm (p/n: PBMK06210) from Merck Milipore (Darmstadt, Germany).

372

373 Liposome batch formulations for characterisation of the Tangential-Flow Filtration (TFF) device

374

375 Multilamellar vesicles (MLV) were prepared using the lipid film hydration method³³. Lipids were weighed and
376 dissolved in a chloroform/methanol (9:1 v/v) mixture. Cationic liposomes comprised DDA:TDB (8:1 molar
377 ratio) and anionic liposomes comprised DPPG, DPPC, Chol (1:1:1.3 molar ratio). The organic solvent was
378 subsequently removed by rotary evaporation under vacuum (100 RPM, 180 mBar, Rotavapor R-100, BÜCHI
379 Labortechnik AG, Switzerland), followed by flushing with nitrogen for removal of solvent residues (5 minutes).
380 The thin lipid film on the bottom of a round bottom flask was hydrated with 10 mM pH 7.2 TRIS buffer. Small
381 liposomes were formed via probe sonication (Soniprep150plus, MSE, UK; 5 min at amplitude of 5). Ethanol
382 was manually added to the liposome formulation to a final concentration of 20% (v/v) to simulate solvent
383 contents commonly resulting from the microfluidics production method. Ovalbumin (100 $\mu\text{g mL}^{-1}$) was used
384 as a model protein, and propofol (1 mg mL^{-1}) as a model drug. These were added to the liposome
385 formulation post-production to mimic the conditions post liposome manufacturing by microfluidics.

386

387 Device fabrication

388

389 As previously reported, the filtration system was designed to seal membranes in place by means of
390 mechanical clamping²⁴. Two poly(methylmethacrylate) (PMMA) plates, with a straight channel (1 mm width, 1
391 mm depth, 45 mm length) and a 1 mm hole milled at each end were clamped together using M3 screws
392 along the edges (Torque 10 Ncm). A 1 mm wide and 0.75 mm deep cutting was used to hold the PDMS
393 gasket in place, which was used to secure the membrane in place (Supplementary Figure S4). Different
394 commercially available membrane sheets were cut to the required size using a CO₂ laser marking head
395 (Synrad Inc., Mukilteo, WA, USA). The membranes used in this set of experiments had a cut-off of 10kDa or
396 300kDa, for drug or protein filtration, respectively. The membranes were cleaned after each experiment by
397 back-flushing with water and stored inside the TFF system in 0.8 M saline solution, ready for the next
398 experiment.

399

400 Additionally, a clamping system was made from PMMA (two plates held together by screws [M3]) for the
401 staggered herringbone micromixer (SHM) chip using a micromilling machine (M3400E, Folken IND,
402 Glendale, USA). The gasket for the filtration unit was manufactured from poly(dimethylsiloxane) (PDMS,
403 Sylgard 184, Dow Corning, Midland, USA), according to the manufacturer's instructions and cast in PMMA
404 moulds, manufactured as described above. Interconnect ports (milled from 5 mm PMMA), with two holes
405 tapped with an M3 thread were used for connection to the filtration unit; an M6 threaded hole was used for
406 standard connection fittings (P-221, Upchurch Scientific, Oak Harbor, WA, USA).

407

408 Backpressure regulation

409

410 Backpressures were regulated through capillaries, which were attached to the retentate outlet of the filtration
411 device (see Supplementary Fig. S3 online). These capillaries restricted the flow as they were selected with
412 internal diameters smaller than the polytetrafluoroethylene (PTFE) tubing (1/16 in. x 0.031 in., p/n: 58700-U,
413 Sigma- Aldrich Int.) which connected the TFF device with auxiliary pumps and collection vials. Backpressure
414 was calculated using Hagen-Poiseuille's Law

415

$$\Delta P = \frac{128 \cdot \mu \cdot L \cdot Q}{\pi \cdot D^4} \quad (1)$$

416
417
418
419
420
421
422
423
424
425
426
427
428
429
430
431
432
433
434
435
436
437
438
439
440
441
442
443
444
445
446
447
448
449
450
451
452
453
454
455
456
457
458
459
460
461
462
463
464
465
466
467
468
469
470
471
472
473
474
475

where μ , L , d and Q are the dynamic viscosity of the medium at 25 °C, the length and internal diameter of the restricting capillary, and the volumetric flow rate, respectively. We used Hagen-Poiseuille's equation (1) to select the capillary sizes and the flow rates to attain the backpressure range from 5 to 80 psi. For each backpressure analysis, a capillary was connected to the TFF retentate outlet using PTFE tubing, ferrules (p/n: P-200, IDEX Europe GmbH, Germany) connectors (Flangeless Nuts, p/n: P-247, PEEK, M6 Flat-Bottom, for 1/16 in. OD, IDEX Europe GmbH, Germany) and metric unions (Metric Union, M6 Port, p/n: P-602, IDEX Europe GmbH, Germany). The inlet of the TFF was connected through a Luer-lock fitting and polytetrafluoroethylene PTFE tubing to a single-use plastic syringe. Water was fed in the TFF device at discrete flow rates ranging from 0.01 to 2.5 mL min⁻¹ attained by a syringe pump (Nemesys, Cetoni GmbH, Germany). Backpressures were measured experimentally with a pressure sensor (40PC100, Honeywell, NJ, USA) connected on the retentate side; the data was logged with a LabVIEW virtual instrument (National Instruments, TX, USA). We compared the theoretical backpressures from equation (1) to the measured backpressures, and the measured values exceeded their calculated counterparts from 20% to 6.25% when increasing the applied backpressure from 5 to 80 psi, respectively (Supplementary Figure S5, and Supplementary Table S6). One of the TFF outlets was intentionally sealed with a flat bottom plug (p/n: P-314, M6, IDEX Europe GmbH, Germany) while a single outlet connected through a ferrule (p/n: P-200), nut (p/n: P-247) and tubing into a collection vial for liquid passing through the membrane.

Filtration

Filtration was performed in diafiltration mode to investigate the liposome behaviour in the established pressure and flow rate range (Table 2). For this experiment, bench-top prepared liposomes in aqueous solution were spiked with drug, protein or solvent, and were introduced into the TFF by means of syringe pumps (Nemesys, Cetoni GmbH, Germany), connectors and capillaries as described earlier. A capillary was connected to the TFF, in *cis*-configuration (on the same side of the membrane), and closed the loop of the retentate fluidic line (see Supplementary Fig. S3 online). Retentate from the TFF was collected in an intermediate collection vial and could be injected in the device hence allowing for multiple passes, referred in this article as diafiltration cycles. Transmembrane pressure was attained by controlling the flow rates in the pump; also by adding a constriction capillary of known geometry, *i.e.* internal diameter and length. Retentate and permeate fractions were collected in Eppendorf tubes, assessed by weight, and used for further analysis, *i.e.* zeta potential, size, polydispersity, quantification via HPLC. A volume of TRIS buffer, 10 mM pH 7.2, was added after each diafiltration cycle to compensate for the amount of liquid passing through the membrane (in permeate) and to sustain steady concentration levels (in retentate) during the continuous purification process.

Continuous process flow configuration

To test the continuous processing of liposome formation followed by liposome purification, a SHM and a TFF device were connected in sequence. The SHM (Precision Nanosystems Inc., Vancouver, Canada) consisted of two inlets, a bifurcated channel with herringbone structures, and single outlet moulded in PDMS. The channels were 200 μ m in width and 79 μ m in height with herringbone features of 50 μ m in width, 31 μ m in height, 45° angle, asymmetry index 2:1 (according to Precision Nanosystems, Inc.). Luer-lock fitting and polytetrafluoroethylene (PTFE) tubing (1/16 in. x 0.031 in., Sigma- Aldrich Int.) were used to link disposable 1 mL syringes with the two inlet ports of the chip; flow rates and flow rate ratios were controlled by syringe pumps (Nemesys, Cetoni GmbH, Germany) and the whole system was primed with Tris buffer (10 mM, pH 7.2) prior to operation. Organic phase, a weighed amount of lipids in ethanol, was injected into the first inlet of the SHM device, while in the second inlet aqueous phase (TRIS buffer, 10mM, pH 7.2) was injected. The micromixer was held in place using a clamping device made out of PMMA. The micromixer was connected to the tangential flow filtration unit *via* an intermediate collection vial (2.0 mL Eppendorf) for additional functionality. This allows the addition of various components such as of microfluidics-manufactured liposomes prior to the filtration system for purification. A bi-directional milliGAT pump (VICI Valco, Valco Instruments Co.) was connected in-line with the retentate loop of the TFF through a capillary at the bottom of that intermediate collection vial. Transmembrane pressures was varied by restricting the flow of the retentate using different small diameter capillaries connected in-line with the TFF outlet. The retentate flowed through the capillary and was collected in the intermediate vial, while permeate passed through the membrane and was gathered in a separate tube. Both fractions were analysed for content of liposomes, propofol, protein, lipid and ethanol.

Two different liposome formulations were produced using the coupled SHM to TFF systems. For the

476 preparation of neutral liposomes, PC and Chol (4:1 molar ratio) in ethanol were injected into the micromixer
477 at a total flow rate (TFR) of 2 mL min⁻¹ and a flow rate ratio (FRR) of 1:3; bilayer drug loading was achieved
478 by including 1 mg mL⁻¹ of propofol in the solvent stream. For the preparation of a cationic liposome
479 formulation, DOPE and DOTAP (1:1 molar ratio) in ethanol were injected into the micromixer at a TFR of 2
480 mL min⁻¹ at FRR 1:3. After formulation, the required amount of protein (ovalbumin, 100 µg mL⁻¹) was added
481 to the intermediate collection vial. Manually adding fresh solution to the intermediate collection vial
482 compensated for liquid passing through the membrane into permeate. Otherwise, the amount of the fluid in
483 the system would fall below a critical level and purification would need to be interrupted because of
484 insufficient circulating liquid volume.

485 486 **Measurement of particle characteristics**

487
488 Nanoparticle tracking analysis (NTA) was performed with a Nanosight LM20 (NanoSight, Amesbury, UK),
489 connected to a microscope (with 20× magnification). Liposomes were diluted 1:10 to 1:100 in distilled water,
490 to achieve an optimal particle concentration of 10⁷ – 10⁹ particles/mL during measurement. NTA analysis
491 was used to determine the particle concentration per millilitre (P/mL), recording time was 60 seconds and
492 camera settings (shutter and gain) were adjusted manually to maximise resolution. Dynamic light scattering
493 (DLS) (Malvern Zetasizer Nano-ZS, Malvern Instruments, Worcestershire, UK) was used to report the z-
494 average (intensity based mean particle diameter), and to report the polydispersity (PDI), in order to assess
495 the width of the particle distribution. Liposomes were diluted 1:10 in distilled water and measurements took
496 place at 25°C. Zeta potential (ZP) was measured using particle electrophoresis (Malvern NanoZS, Malvern
497 Instruments, Worcestershire, UK).

498 499 **Propofol quantification**

500
501 Quantification of propofol was performed by reverse phase HPLC (Luna 5µ C18, Phenomenex, UK, pore
502 size of 100Å, particle size of 5 µm) at 268 nm. The flow rate was constant at 1 mL min⁻¹ throughout with a
503 gradient elution from 5:95 (Methanol: 0.1% Trifluoroacetic Acid, TFA, in water) to 100:0 (Methanol: 0.1% TFA
504 in water) over 10 minutes. HPLC-grade solvents were used, sonicated and filtered. The column temperature
505 was controlled at 35°C. All analysis was made with Clarity, DataApex, version 4.0 (DataApex, Prague, Czech
506 Republic). For quantification, established calibration curves of propofol were used as reported previously¹⁴.

507 508 **Protein and lipid quantification**

509
510 Samples were loaded on a HPLC and elution was performed with a gradient from 5:95 to 100:0 (Methanol:
511 0.1% TFA in water) over 20 and 40 minutes for protein and lipid detection, respectively. Quantification was
512 performed by an evaporative light scattering detector (ELSD) (Sedex 90, Sedere, France), set at 52°C and
513 coupled to the HPLC as described previously¹⁸. A calibration curve was established from standards
514 (ovalbumin in TRIS buffer, pH 7.2, lipids in ethanol) in six replicates at concentrations from 5 to 100 µg mL⁻¹
515 (protein) and 0.05 to 1.5 mg mL⁻¹ (lipids).

516 517 **Ethanol quantification**

518
519 Solvent concentration was quantified by gas chromatography (GC) using a flame ionization detector (CSI
520 200 Series, column TRACE 15 m x 0.25 mm x 0.25 µm TR-5, Thermo Scientific, UK), with detector
521 temperature 230°C, injector temperature 200°C and an injection volume of 1 µL. The carrier gas was helium
522 at 15 psi inlet pressure. A calibration curve (6 standards ranging from 0.5-50% v/v) was established and
523 used for quantification using an internal reference standard (propan-1-ol). All analysis was made in Clarity
524 DataApex version 2.4 (see above).

525 526 **Statistical analysis**

527
528 Unless stated otherwise, results were reported as the mean ± one standard deviation (SD., n=3). One- or
529 two-way analysis of variance (ANOVA) was used to assess statistical significance, followed by Tukey's
530 multiple comparing test (post-hoc analysis). A t-test was performed for paired comparisons. Significance was
531 acknowledged for p values lower than 0.05, marked with and asterisk (*). All calculations were made in
532 GraphPad Prism version 6.0 (GraphPad Software Inc., La Jolla, CA, US).

533 534 535 **References**

536
537 1. Carugo, D., Bottaro, E., Owen, J., Stride, E., & Nastruzzi, C. Liposome production by microfluidics:
538 potential and limiting factors. *Scientific Reports* 6, (25876):25876 (2016).
539
540 2. Mayer, L. D., Hope, M. J., & Cullis, P. R. Vesicles of variable sizes produced by a rapid extrusion
541 procedure. *Biochimica et Biophysica Acta* 858, 161-68 (1986).
542
543 3. Hinna, A., Streiniger, F., Hupfeld, S., Stein, P., Kuntsche, J., & Brandtl, M. Filter-extruded liposomes
544 revisited: a study into size distributions and morphologies in relation to lipid-composition and process
545 parameters. *J. Liposome Research* 26 (1), 11-20 (2014).
546
547 4. Gregoriadis, G., Liposome preparation and related techniques in Liposome Technology 2nd ed., Vol. 1 (ed.
548 Gregoriadis, G.) 50-65 (CRC Press Inc., 1992).
549
550 5. Zhigaltsev, I. V., Belliveau, N., Hafez, I., Leung, A. K., Huft, J., Hansen, C., & Cullis, P. R. Bottom-up
551 design and synthesis of limit size lipid nanoparticle systems with aqueous and triglyceride cores using
552 millisecond microfluidic mixing. *Langmuir* 28 (7), 3633-40 (2012).
553
554 6. Jahn, A., Stavis, S.M., Hong, J.S., Vreeland, W.N., DeVoe, D.L., & Gaitan, M. Microfluidic mixing and the
555 formation of nanoscale lipid vesicles. *ACS Nano* 4 (4), 2077-87 (2010).
556
557 7. Jahn, A., Vreeland, W. N., DeVoe D. L., Locascio L. E., & Gaitan, M. Microfluidic directed formation of
558 liposomes of controlled size. *Langmuir* 23 (11), 6289-93 (2007).
559
560 8. Demello A. J. Control and detection of chemical reactions in microfluidic systems. *Nature* 442 (7101), 394-
561 402 (2006).
562
563 9. Song Y., Hormes J., & Kumar, C.S. Microfluidic synthesis of nanomaterials. *Small* 4 (6), 698-711 (2008).
564
565 10. Schroën, K., Bliznyuk, O., Muijlwijk, K., Sahin, S., & Berton-Carabin, C. C. Microfluidic emulsification
566 devices: from micrometer insights to large-scale food emulsion production. *Current Opinion in Food Science*
567 3, 33-40 (2015).
568
569
570 11. van Swaay, D. Microfluidic methods for forming liposomes. *Lab on a Chip* 13 (5), 752-767 (2013).
571
572 12. Bleul, R., Thiermann, R., & Maskos, M. Techniques to control polymersome size. *Macromolecules* 48,
573 7396-7409, (2015).
574
575 13. Ghazal, A., Gontsarik, M., Kutter, J. P., La, J. P., Ahmadvand, D., Labrador, A., & Yaghmur, A.
576 Microfluidic platform for the continuous production and characterization of multilamellar vesicles: A
577 synchrotron small- angle X - ray scattering (SAXS) study. *J. Phys. Chem. Lett.* 8, 73-79 (2017).
578
579 14. Pattni, B. S., Chupin, V. V., & Torchilin, V. P. New developments in liposomal drug delivery. *Chemical*
580 *Reviews* 115(19), 10938-10966 (2015).
581
582 15. He, J., Wang, L., Wei, Z., Yang, Y., Wang, C., Han, X., & Nie, Z. Vesicular self-assembly of colloidal
583 amphiphiles in microfluidics. *ACS Appl. Mater. Interfaces* 5, 9746-9751 (2013).
584
585
586 16. Hood, R. R., & DeVoe, D. L. High-throughput continuous flow production of nanoscale liposomes by
587 microfluidic vertical flow focusing. *Small* 11, (43), 5790-5799 (2015).
588
589 17. Lim, J., Swami, A., Gilson, L. M., Chopra, S., Choi, S., Wu, J., & Arabia, S. Ultra-high throughput
590 synthesis of nanoparticles with homogeneous size distribution using a coaxial. *ACS Nano* 8 (6), 6056-6065
591 (2014).
592
593
594 18. Kastner, E., Verma, V., Lowry, D., & Perrie, Y. Microfluidic-controlled manufacture of liposomes for the
595 solubilisation of a poorly water soluble drug. *Int J Pharmaceutics* 485 (1), 122-130 (2015).

- 596
597 19. Wagner, A., Vorauer-Uhl, & K., Katinger, H. Liposomes produced in a pilot scale: production, purification
598 and efficiency aspects. *Eur. J. Pharmaceutics Biopharmaceutics* 54 (2), 213-219 (2002).
599
- 600 20. Pattnaik, P., Ray, T. 2009. Improving liposome integrity and easing bottlenecks to production.
601 *Pharmaceutical Technology Europe* 22 (6), 24-28 (2009).
602
- 603 21. Ruyschaert, T., Marque, A., Duteyrat, J. L., Lesieur, S., Winterhalter, M., & Fournier D. Liposome
604 retention in size exclusion chromatography. *BMC Biotech* 5 (1), 11 (2005).
605
- 606 22. Hood, R., Vreeland, W., & DeVoe, D. Microfluidic remote loading for rapid single-step liposomal drug
607 preparation. *Lab Chip* 14 (17), 3359-3367 (2014).
608
- 609
- 610 23. Belliveau, N. M., Huft, J., Lin, P. J., Chen, S, Leung, A. K., Leaver, T. J., Wild, A. W., Lee, J. B., Taylor,
611 R. J., & Tam, Y. K. Microfluidic synthesis of highly potent limit-size lipid nanoparticles for in vivo delivery of
612 siRNA. *Mol Therapy Nuc Acids* 1 (8), e37 (2012).
613
- 614 24. O'Sullivan, B., Al-Bahrani, H., Lawrence, J., Campos, M., Cázares, A., Baganz, F., Wohlgemuth, R.,
615 Hailes H. C., & Szita N. Modular microfluidic reactor and inline filtration system for the biocatalytic synthesis
616 of chiral metabolites. *J Mol Catalysis B: Enzymatic* 77, 1-8 (2012).
617
- 618 25. Kastner, E., Kaur, R., Lowry, D., Moghaddam, B., Wilkinson, A., & Perrie, Y. High-throughput
619 manufacturing of size-tuned liposomes by a new microfluidics method using enhanced statistical tools for
620 characterization. *Int J Pharmaceutics* 477, (1-2):361-8 (2014).
621
- 622 26. van Reis, R., & Zydney, A. Bioprocess membrane technology. *J Memb Sci.* 297 (1), 16-50 (2007).
623
- 624 27. Tomotaka, N., & Makoto, Y. Mechanosensitive liposomes as artificial chaperones for shear-
625 driven acceleration of enzyme-catalyzed reaction. *ACS Appl. Mater. Interfaces* (6), 3671–3679 (2014).
626
- 627 28. Cullis, P. R., Hope, M. J., & Bally, M. B. Extrusion technique for producing unilamellar vesicles. In Google
628 Patents: 1991.
629
- 630 29. Hansch, C., Leo, A., & Hoekman, D. Exploring QSAR: Hydrophobic, electronic, and steric constants. (ed.
631 Hansch, C., Leo, A., Hoekman, D. H.) 105 (*Washington DC: American Chemical Society*, 1995).
632
- 633 30. Kaur, R., Henriksen-Lacey, M., Wilkhu, J., Devitt, A., Christensen, D., & Perrie, Y. Effect of incorporating
634 cholesterol into DDA: TDB liposomal adjuvants on bilayer properties, biodistribution, and immune responses.
635 *Mol Pharmaceutics* 11, (1), 197-207 (2013).
636
- 637 31. Mithun, M., Saumyabrata, M., Souparno, B., Somsubhra, T. C., Abdus, S., Md S., Pradyot, B., & Nahid,
638 A. A lipid based antigen delivery system efficiently facilitates MHC class-I antigen presentation in dendritic
639 cells to stimulate CD8+ T cells. *Scientific Reports* (6), 27206 (2016).
640
- 641 32. Ball, P. Scale-up and scale-down of membrane-based separation processes. *Memb Technology* (117),
642 10-13 (2000).
643
- 644 33. Bangham, A., Standish, M. M., & Watkins, J. Diffusion of univalent ions across the lamellae of swollen
645 phospholipids. *J Mol Bio.* 13, (1), 238-IN27 (1965).
646
- 647 34. Smith Korsholm, K., Agger, E. M., Foged, C., Christensen, D., Dietrich, J., Andersen, C. S., Geisler, C., &
648 Andersen, P. The adjuvant mechanism of cationic dimethyldioctadecylammonium liposomes. *Immunology*
649 121, (2), 216-226 (2007).
650
- 651 35. Christensen, D., Agger, E. M., Andreasen, L. V., Kirby, D., Andersen, P., & Perrie Y. Liposome-based
652 cationic adjuvant formulations (CAF): past, present, and future. *J Liposome Research* 19, (1), 2-11 (2009).
653
- 654 36. Henriksen-Lacey, M., Christensen, D., Bramwell, V. W., Lindenstrøm, T., Agger, E. M., Andersen, P., &
655 Perrie, Y. Comparison of the depot effect and immunogenicity of liposomes based on

- 656 dimethyldioctadecylammonium (DDA), 3 β -[N-(N', N'-dimethylaminoethane) carbonyl] cholesterol (DC-Chol),
657 and 1, 2-dioleoyl-3-trimethylammonium propane (DOTAP): prolonged liposome retention mediates stronger
658 Th1 responses. *Mol Pharmaceutics* 8, (1), 153-161 (2010).
659
- 660 37. Senior, J., & Gregoriadis, G. Stability of small unilamellar liposomes in serum and clearance from the
661 circulation: the effect of the phospholipid and cholesterol components. *Life Sciences* 30, (24), 2123-2136
662 (1982).
663
- 664 38. Gregoriadis, G., & Senior, J. The phospholipid component of small unilamellar liposomes controls the
665 rate of clearance of entrapped solutes from the circulation. *FEBS Letters* 119, (1), 43-46 (1980).
666
- 667 39. Oku, N., Namba, Y., & Okada S. Tumor accumulation of novel RES-avoiding liposomes. *Biochimica*
668 *Biophysica Acta (BBA)-Lipids and Lipid Metabolism* 1126, (3), 255-260 (1992).
669
- 670 40. Kirby, C., Clarke, J., & Gregoriadis, G. Effect of the cholesterol content of small unilamellar liposomes on
671 their stability in vivo and in vitro. *Biochem J.* 186, 591-598 (1980).
672

673 Acknowledgements

674
675 This work was part funded by the EPSRC Centre for Innovative Manufacturing in Emergent Macromolecular
676 Therapies and Aston University. This research was made possible with the financial support from BBSRC
677 (BB/L000997/1) and the European Research Area initiative on industrial biotechnology (ERA-IB; third joint
678 call). The Authors have no conflict of interest to declare. We would like to kindly thank Dr Manni Bhatti from
679 UCL for her help in proofreading the manuscript.
680

681 Author contributions statement

682
683 N.D., E.K. and M.H. conceived and conducted the experiments, N.D., E.K., Y.P., N.S. analysed the results
684 and reviewed the manuscript.
685

686 Additional information

687
688 The authors have no conflict of interest to declare.
689

690 **Figure 1:** Particle size and polydispersity as a function of increasing backpressures in the TFF system as
691 collected on the retentate side of the membrane. Images from NTA analysis, verifying particles in permeate
692 (top) and retentate (bottom) stream at increasing backpressures. Particles were found in the permeate at
693 backpressures exceeding 75 psi. All experimental datasets are presented as mean and standard deviation
694 (mean \pm s.d.) resulting from three independent runs (n=3).

695 **Figure 2:** (a) Vesicle size, polydispersity (PDI), zeta potential (ZP) and particle concentration (P/mL) for
696 cationic (DDA:TDB) and anionic (DPPG:DPPC:Chol) liposomes before and after the TFF purification. (a)
697 Images from NTA show vesicles present in the retentate side only. (c) Propofol and ethanol removal achieved
698 over three diafiltration cycles for anionic liposomes (DPPG:DPPC:Chol), expressed as a percentage of the
699 initial amount of contaminants present.

700 **Figure 3:** Vesicle size, polydispersity (PDI), zeta potential (ZP) and particle concentration (P/mL) for (a)
701 anionic liposomes (DPPG:DPPC:Chol) and (b) cationic liposomes (DDA:TDB) prior and post OVA-addition
702 (ovalbumin, 100 $\mu\text{g mL}^{-1}$), and particle characteristics after the TFF purification. Protein (ovalbumin) and
703 ethanol removal achieved over three diafiltration cycles for (c) anionic and (d) cationic liposomes, expressed
704 as a percentage of the initial amount of contaminants present. All experimental datasets are presented as
705 mean and standard deviation (mean \pm s.d.) average of three independent runs (n=3).

706 **Figure 4:** (a) Schematic overview of the module-based microfluidic system. Liposomes were manufactured
707 with a **Staggered Herringbone Mixer** (SHM) upstream and flowed through the **Tangential Flow Filtration**
708 (TFF) device for consecutive purification. (b) Schematic overview of the formation of liposomes loaded with a
709 low-solubility model drug, *i.e.* propofol. Vesicle assembly and drug loading are performed with a SHM, and

710 non-entrapped (free) drug is removed from the mixture by consecutive filtration inside the TFF system. (c)
 711 Schematic overview of the formation of liposomes loaded with a model protein, ovalbumin (OVA). Vesicle
 712 assembly is performed with a SHM, with post-assembly protein addition; non-entrapped (free) protein is
 713 removed by consecutive diafiltration cycles inside the TFF system.

714 **Figure 5:** Lipid recovery in the continuous liposome factory-on-a-bench for (a) lipid recovery after four
 715 diafiltration cycles. (b) Lipid concentration in four concentration cycles, related to the initial amount of lipids
 716 present prior to the concentration cycles. All experimental datasets are presented as mean and standard
 717 deviation (mean \pm s.d.) average of three independent runs (n=3).

718

719 **Table 1: Lipids investigated in this study.**

Lipid	Application	Reference
Dimethyldioctadecyl ammonium bromide (DDA)	Vaccine adjuvant, cationic head group Uptake of vaccine antigens to antigen presenting cells	Smith Korsholm et al. ³⁴ Christensen et al. ³⁵
Trehalose 6,6-dibehenate (TDB)	Synthetic immunostimulator derived from the membrane of mycobacterium	
1,2-dioleoyl-sn-glycero-3-phosphoethanolamine (DOPE)	Fusogenic helper lipid, available in the commercial Lipofectin™ transfection reagent	Henriksen-Lacey et al. ³⁶
1,2-dioleoyl-3-trimethylammonium-propane (DOTAP)	Cationic lipid often used in transfection	
Egg Phosphatidylcholine (PC)	Neutral head group, drug delivery	Senior and Gregoriadis ³⁷ Gregoriadis and Senior ³⁸
1,2-Dipalmitoyl-sn-glycero-3-phospho- <i>rac</i> -(1-glycerol) (DPPG)	Negative charged head group drug delivery	Oku et al. ³⁹ Kirby et al. ⁴⁰
1,2-Dipalmitoyl-sn-glycero-3-phosphocholine (DPPC)	Neutral head group, drug delivery	
Cholesterol (Chol)	Added for membrane stabilization, known to effect drug encapsulation efficiency in bilayer and aqueous core	Senior and Gregoriadis ³⁷ Kirby et al. ⁴⁰

720

721

722

723 **Table 2: Backpressures and flow rates through the Tangential Flow Filter (TFF) that were investigated in this study.**
 724 Liposomes in solution were fed into the TFF device at flow rates ranging between 0.01 and 2.5 mL min⁻¹. Backpressure
 725 was attained by connecting a restrictive capillary with selected (I.D.) and/or length on the retentate side of the TFF
 726 outlet.

Backpressure (psi) 7 15 23 31 39 49 50 59 62 75 80

Flow rate (mL min ⁻¹)	0.01	0.02	0.03	0.1	0.05	1	0.3	2	2.5	0.5	0.1
Capillary I.D. (μm)	50	50	50	63	50	100	63	100	100	63	50
Capillary length(mm)	50	50	50	50	50	50	25	30	25	25	50

727

728

729

730 **Table 3: Continuous purification of PC:Chol liposomes loaded with propofol.** Propofol and lipids were included in the
 731 ethanol stream. Liposome formation and drug encapsulation was performed in a staggered herringbone mixer (SHM),
 732 operated with a total flow rate of 2mL min⁻¹ and a ratio of 1:3 ethanol:aqueous solution. The results are presented as
 733 mean and standard deviation (mean ± s.d.) resulting from three independent runs (n=3), N/A = not applicable.

	Liposome with drug after SHM	Liposome with drug after three passes through the TFF*
Size (nm)	51.4 ± 2.1	61.2 ± 13.2
Polydispersity	0.29 ± 0.013	0.33 ± 0.09
Loading (mol%)	N/A	51.0 ± 4.0
Effec. ethanol (% v/v)	16.1 ± 3.9	3.1 ± 1.5

734 *After each pass a volume of pure buffer was added to compensate for permate and maintain constant volume of retentate.

735

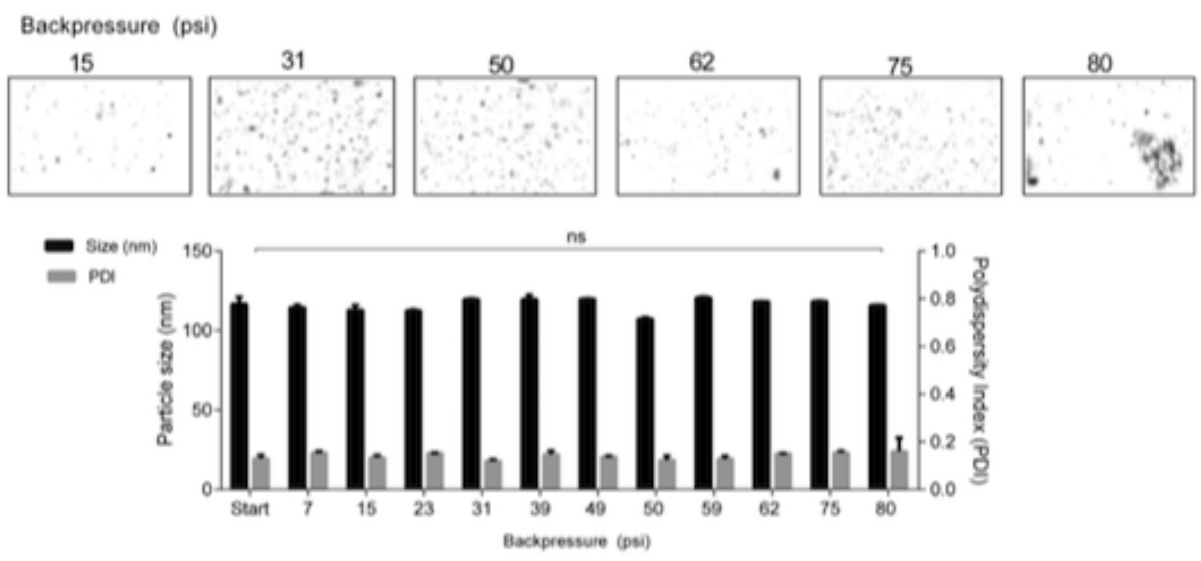
736

737 **Table 4: Continuous purification of DOPE:DOTAP liposomes loaded with protein (ovalbumin).** The lipids were
 738 included in the ethanol stream and liposome formation was performed in a SHM, operated at 2mL min⁻¹ and a ratio of
 739 1:3 solvent:aqueous solution. Protein was added post-liposome formation. OVA = ovalbumin, N/A = not applicable.

	Liposome w/o OVA after SHM	Liposome with OVA in collection vial	Liposome with OVA after three passes through TFF*
Size (nm)	62.8 ± 1.9	88.5 ± 5.7	89.3 ± 10.9
Polydispersity	0.44 ± 0.02	0.45 ± 0.008	0.42 ± 0.02
Zeta potential (mV)	83.9 ± 3.5	43.6 ± 1.6	69.2 ± 6.1
Loading (%)	N/A	N/A	23.9 ± 0.8
Effec. ethanol (% v/v)	N/A	15.0 ± 6.9	4.1 ± 1.5

740 *After each pass a volume of pure buffer was added to the retentate, keeping the level of liquid constant.

Figure 1 A



B

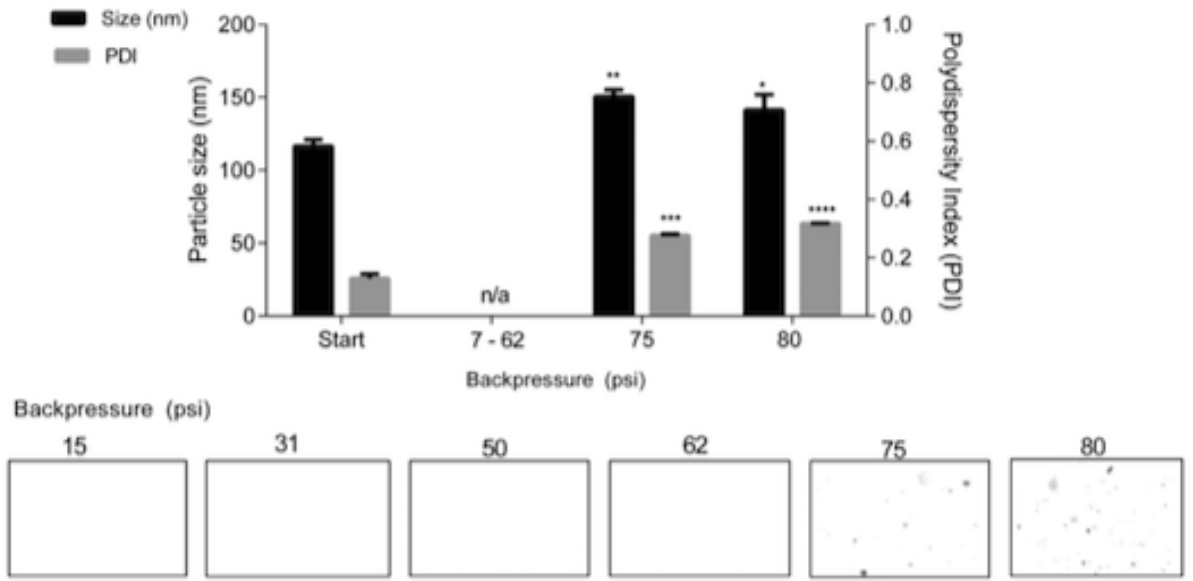


Figure 2

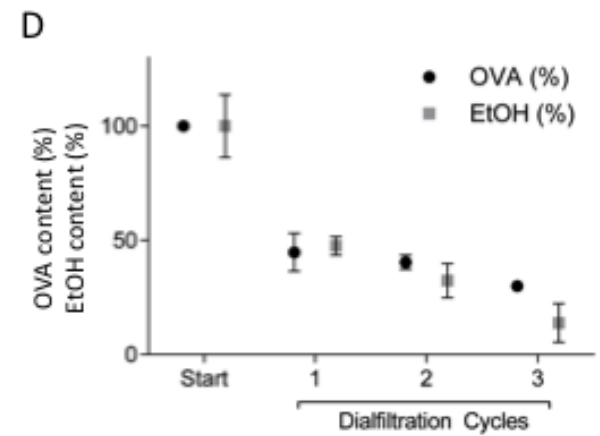
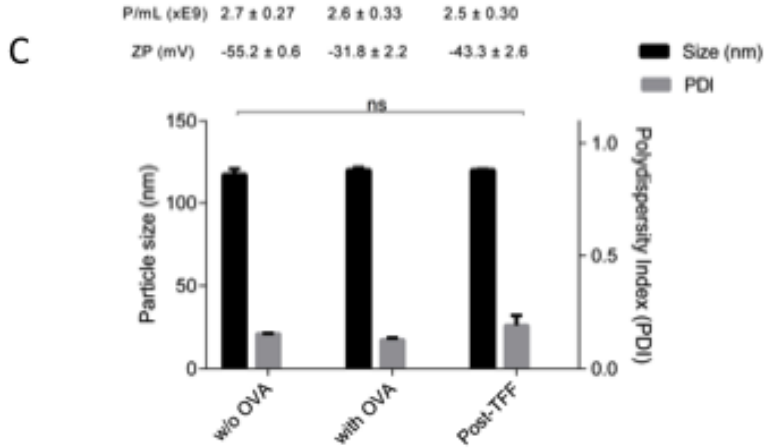
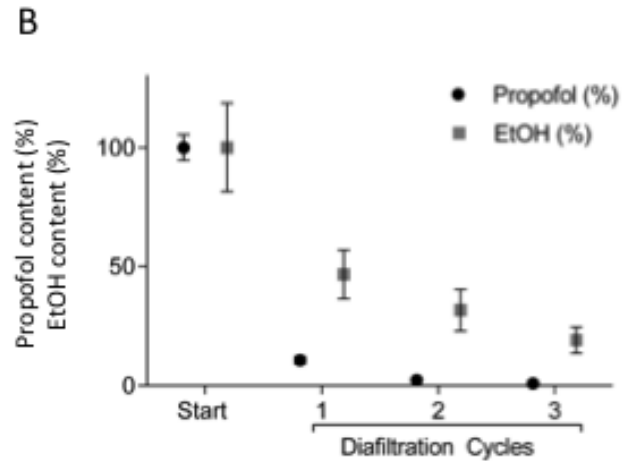
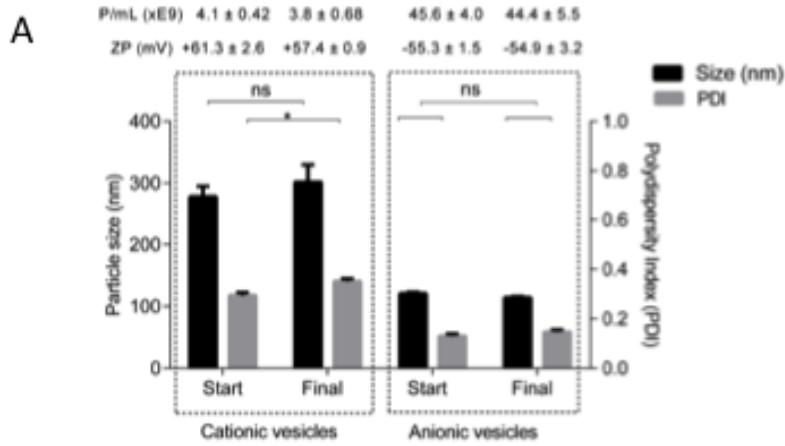


Figure 3

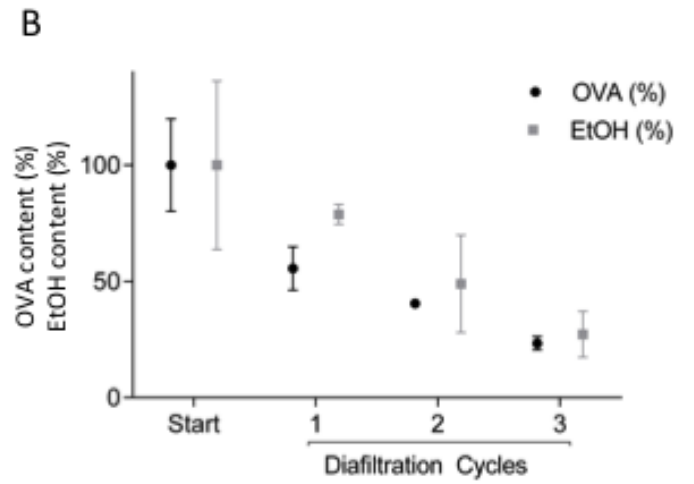
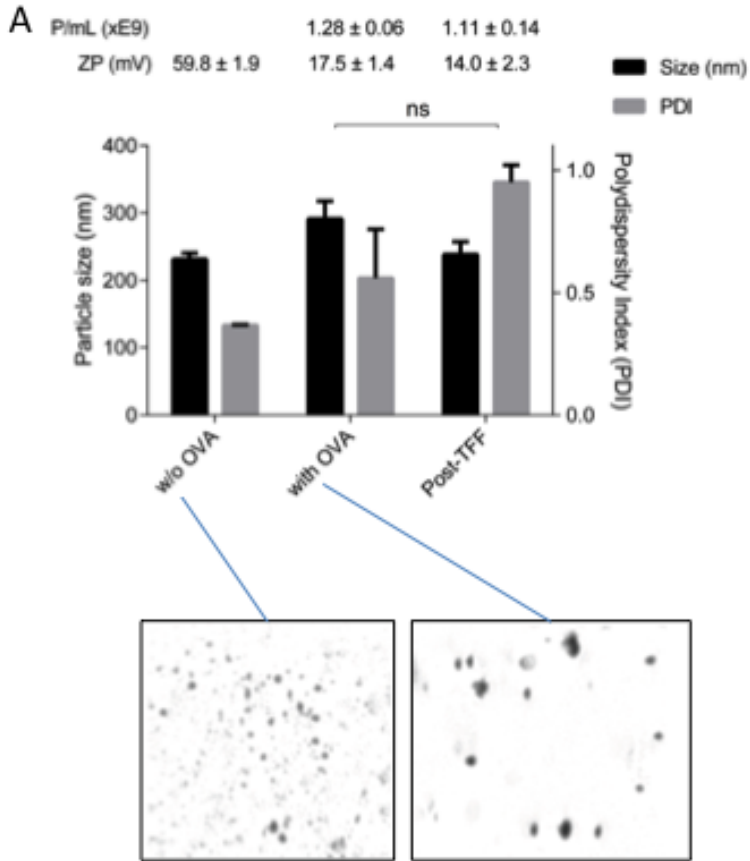


Figure 4

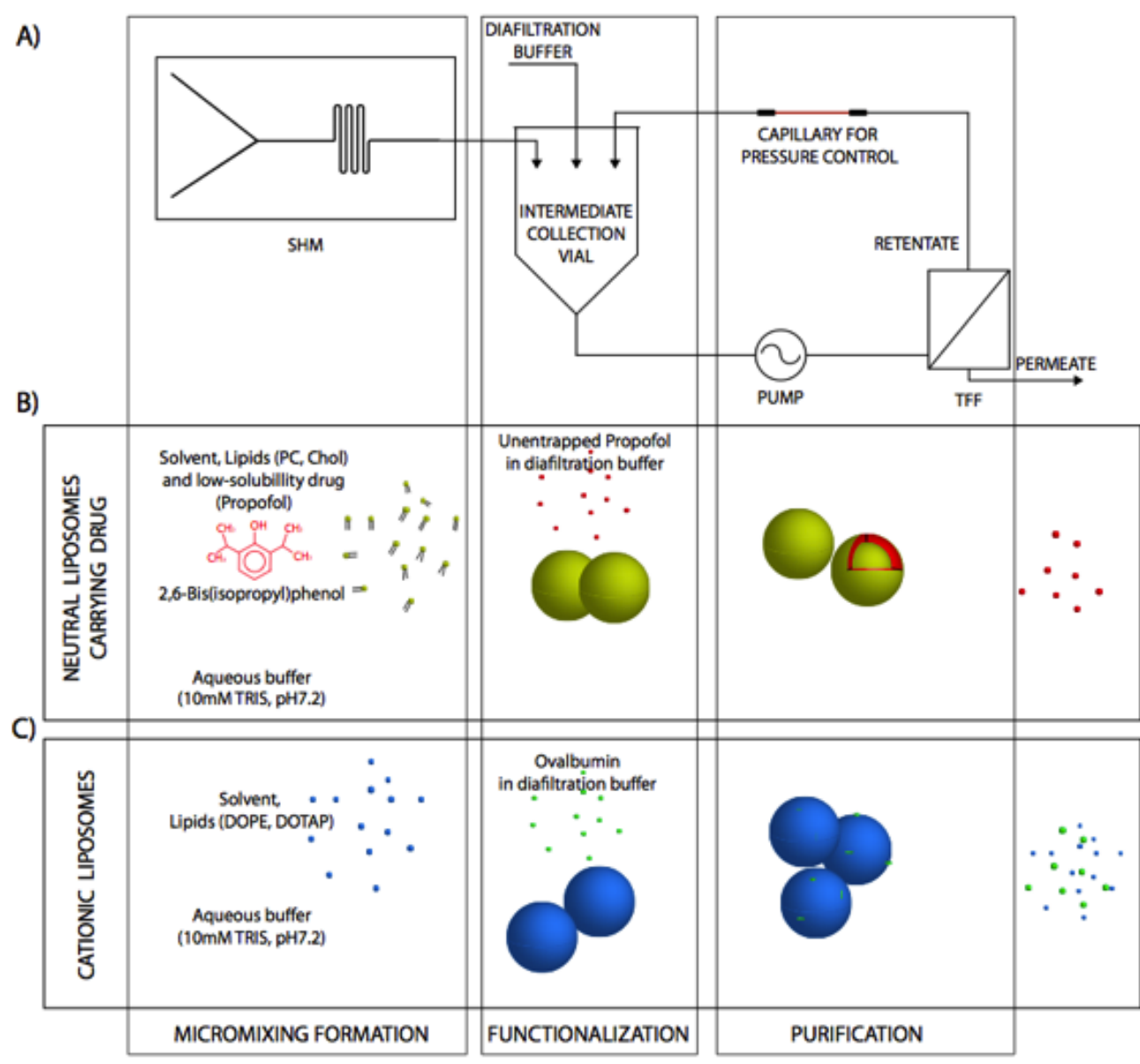
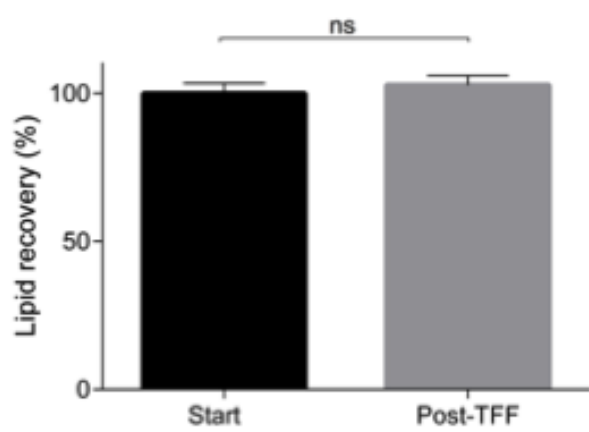


Figure 5

A



B

